Australasian Plant Pathology (2021) 50:203–215
https://doi.org/10.1007/s13313-020-00763-z

ORIGINAL PAPER

Leaf anatomical aspects of CABMV infection in *Passiflora* spp. by light and fluorescence microscopy

Zanon Santana Gonçalves[1] · Lucas Kennedy Silva Lima[2] · Taliane Leila Soares[3] · Everton Hilo de Souza[1] · Onildo Nunes de Jesus[2]

Received: 19 July 2020 / Revised: 5 November 2020 / Accepted: 23 November 2020 / Published online: 6 January 2021

Abstract

Cowpea aphid-borne mosaic virus (CABMV) is the main pathogen that affects passion fruit, causing woodiness disease in Brazil. The identification of sources of resistance in *Passiflora* is necessary for the development of resistant cultivars. The objective of this work was to evaluate the reaction of eight species of *Passiflora* to CABMV and to verify leaf anatomical changes caused by CABMV. Inoculations were performed and symptoms were evaluated until 55 days after inoculation using a scale ranging from 1 (without symptoms) to 4 (highly susceptible). Simultaneously, leaves from infected and control plants for anatomical analysis were collected. The severity of the disease was calculated using the disease index (DI%) and the means were grouped using the Scott-Knott test. The wild species *Passiflora malacophylla*, *P. setacea* and *P. suberosa* were classified as resistant to CABMV. In contrast, *P. alata* and *P. edulis* were susceptible to the virus, with DI values of 58.2 and 51.9%, respectively. Leaf anatomical changes were more drastic in *P. edulis* and *P. alata*. In *P. edulis*, the infection resulted in changes in the organization of the vascular bundles. Resistant wild species showed few anatomical changes. The resistance found in wild species opens the prospect of performing interspecific crosses.

Keywords Passifloraceae · *Passiflora malacophylla* · Yellow passion fruit · Resistance · Plant-pathogen interaction

Introduction

Brazil is the global leader in the production and consumption of yellow passion fruit (*Passiflora edulis* Sims), with approximately 593,429 metric tons produced in an area of 41,584 hectares (IBGE 2020). However, the occurrence of phytosanitary problems has resulted reduced useful life and low productivity (14.3 t ha^{-1}) of orchards. Among these problems is passion fruit woodiness disease caused by *cowpea aphid-borne mosaic virus* (CABMV). It is considered the main viral disease affecting passion fruit in Brazil (Preisigke et al. 2020). As the name indicates, this virus is disseminated by aphid vectors in a non-circulatory and non-persistent manner (Garcêz et al. 2015; Spadotti et al. 2019). The high incidence of the disease has contributed to reduction of the crop cycle to a maximum of one year in several passion fruit production regions (Garcêz et al. 2015; Santos et al. 2015a, b).

The development of resistant cultivars is the most effective method for production in an area with CABMV. However, until now the available commercial yellow passion fruit (*P. edulis*) cultivars are susceptible to this virus. The identification of resistant species in germplasm banks is essential for the development of cultivars resistant to CABMV. The exploration of sources of resistance in wild species has been used with success in several crops (Rai et al. 2020; Cai et al. 2020; Sade et al. 2020). In the case of passion fruit, some wild species, such as *P. setacea* (Santos et al. 2019; Carvalho et al. 2019; Preisigke et al. 2020) and *P. cincinnata* (Jesus et al. 2016) have been used for introgression of resistant alleles of CABMV in *P. edulis* from interspecific hybridizations followed by backcrossing cycles.

✉ Onildo Nunes de Jesus
onildo.nunes@embrapa.br

[1] Universidade Federal do Recôncavo da Bahia, Campus de Cruz das Almas, Rua Rui Barbosa, 710, 44380-000 Cruz das Almas, Bahia, Brazil

[2] Embrapa Mandioca e Fruticultura, Rua Embrapa, s/n, Chapadinha, Caixa Postal 007, 44380-000 Cruz das Almas, Bahia, Brazil

[3] Universidade Estadual de Feira de Santana, Av. Transnordestina, s/n - Novo Horizonte, 44036-900 Feira de Santana, Bahia, Brazil

Several mechanisms are responsible for genetic resistance to the virus, among which physical barriers stand out, by hindering the establishment of the pathogen, such as the presence of cutin, waxes and cell walls (Boutrot and Zipfel 2017; Gouveia et al. 2017; Andersen et al. 2018; Carvalho et al. 2019). Analysis of anatomical traits is also important for understanding the *Passiflora* spp. x CABMV interaction, by identifying cell structures that hinder the pathogen's establishment. The use of fluorescence microscopy to identify callose, calcium oxalate crystals and the formation of tilose has been used in several species in interactions with different microorganisms (Hinch and Clarke 1982; Chen and Kim 2009; Ellinger and Voigt 2014; Palomares-Rius et al. 2017; Xiao et al. 2018; Lima et al. 2019).

Even in the main commercial species (*P. edulis*), the principal changes that occur with systemic spread of the virus within the plant resulting in leaf damage, such as mosaic symptoms, wrinkling and distortions, are still not fully understood. Therefore, it is necessary to better understand the *Passiflora* spp. x CABMV interaction to elucidate the morphoanatomical changes caused by CABMV and understand the mechanisms of action of this virus, which can shed light on this interaction as well as support control or coexistence strategies of this disease. Thus, the objectives of this study were: *i*) to evaluate the reaction to CABMV in eight species of *Passiflora* spp. under greenhouse conditions; and *ii*) to identify excethe possible leaf anatomical changes in these species at different levels of severity resulting from viral infection of *P. edulis* by means of light and fluorescence microscopy.

Materials and methods

Location of experiment and plant material

The experiment was carried out in the premises of Embrapa Mandioca e Fruticultura, located in the municipality of Cruz das Almas, Bahia, Brazil (12° 40' 39" S, 39° 06' 23" W, 226 m). Eight species of *Passiflora* spp. belonging to the *Passiflora* Germplasm Bank (PGB) of Embrapa were used: *P. edulis* Sims cv. BRS Gigante Amarelo (BRS-GA); *P. alata* Curtis (BGP393); *P. foetida* L. (BGP395); *P. gibertii* N.E.Br. (BGP414); *P. malacophylla* L. (BGP170); *P. setacea* DC. (BGP238); *P. suberosa* L. (BGP014) and *P. subrotunda* Mast. (BGP394).

Seeds (n = 30) of each genotype were soaked in 1.0 mL of the plant regulator GA_{4+7} + N-(phenylmethyl)-aminopurine (Promalin®) at a concentration of 400 mg L^{-1} for 24 hours. After this period, the seeds were distributed in plastic pots with capacity of 1.0 L containing a mixture of coconut fiber and commercial substrate (Vivatto Plus®) in the proportion of 3:1 (v/v) plus 40 g of fertilizer (Osmocote®) for each 10 L of substrate. After seedling emergence (about 40 days after sowing), ten plants with greatest uniformity were selected to compose the experimental test. The plants were kept in a greenhouse with temperature around 28 ± 2 ºC and relative humidity of 75 ± 5%, and irrigation was performed manually daily using a watering can with capacity of 10 L.

Artificial inoculation and transmission electron microscopy (TEM)

The source of the CABMV inoculum was plants of *P. edulis* (susceptible) kept in a greenhouse. The treated plants received mechanical inoculation with CABMV while the plants in the control group did not, 45 days after the emergence of the plants, when they had at least four expanded leaves, following the method described by Gonçalves et al. (2018).

The virus used in the inoculations was obtained from apical leaf tissue of the plants kept in a greenhouse with severe symptoms of CABMV, and was identified by transmission electron microscopy (TEM) (Kitajima et al. 2008) and by RT-PCR in previous studies using the same plant as a source of inoculum (Gonçalves et al. 2018).

Assessment of symptoms and severity of CABMV

The reaction of the eight *Passiflora* species infected with CABMV was characterized based on the visual symptoms of the disease. The evaluations were carried out with the first fully expanded leaf from the apex, by observation of 10 leaves per plant. The first evaluation was performed 20 days after the first inoculation (DAI), and the others at intervals of seven days, ending with the sixth evaluation at 55 DAI. Symptom assessments used a diagrammatic grade scale based on severity levels that ranged from 1 to 4 asymptomatic (level = 1); leaf showing light mosaic (level = 2); leaf showing severe mosaic and blistering (level = 3); leaf showing severe mosaic, blistering and leaf deformations (level = 4), as established by Novaes and Resende (2003) (Fig. 1).

To quantify the severity of the symptoms of CABMV, the disease index (DI) was used (Mckinney 1923) at 55 DAI. This index is calculated based on the weighting of the scale of infection levels, applying the following formula: DI (%) = (GS x L)/ (TNL x HGS); where: GS = degree of scale determined for each leaf; L = number of leaves with each degree of symptoms (level); TNL = total number of leaves evaluated and HGS = maximum degree of infection.

Leaf anatomy

For anatomical analysis, segments of the internervural region (n = 6) were collected from leaves infected with

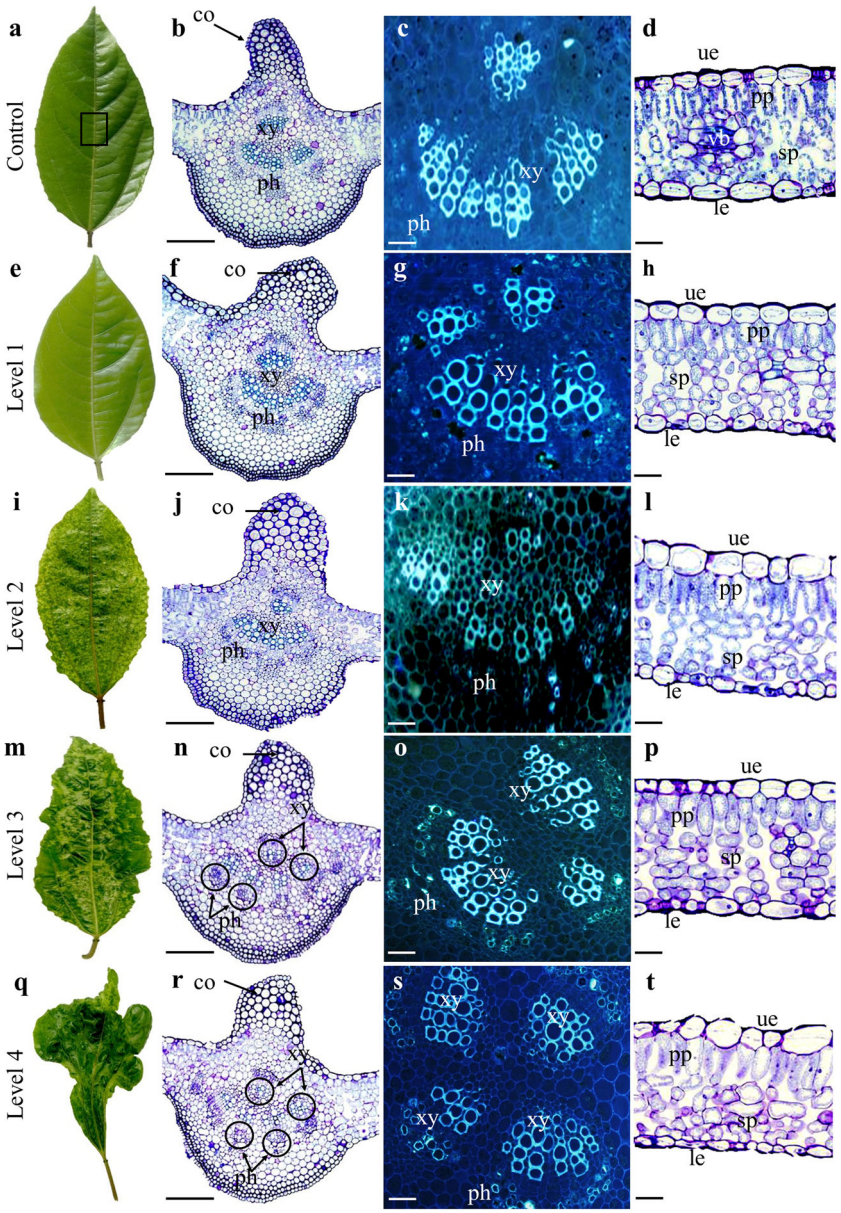

Fig. 1 Light and fluorescence photomicrographs of *P. edulis*. **a-d** healthy leaf (control), the rectangle indicates the internervural region of the *Passiflora* leaf used for anatomical analysis; **e-h** leaf infected with the CABMV and asymptomatic (level = 1); **i-l** infected leaf showing light mosaic (level = 2); m-p) infected leaf showing severe mosaic and blistering (level = 3); **q-t** infected leaf showing severe mosaic, blistering and leaf deformations (level = 4). xy: xylem; ph: phloem; co: collenchyma; ue: upper epidermis; le: lower epidermis: pp: palisade parenchyma; sp: spongy parenchyma; vb: vascular bundle. Bars: 500 µm (b, f, j, n, r); 200 µm (c, d, g, h, k, l, o, p, s, t)

CABMV and the respective controls of the eight *Passiflora* species, mature leaves are selected and fully expanded for all species (Fig. 1, 2, 3, and 4). For *P. edulis*, the leaf segments were collected according to the degree of severity of the symptoms caused by CABMV, according to the scale shown in Fig. 1. The process of fixing, blocking and cutting the samples was performed as described by Lima et al. (2019).

For fluorescence microscopy, the leaf segments were stained with Lugol's iodine for 3 min, then washed with tap water and stained with 1% aniline for 8 min and finally in Lugol again for 30 s. The slides were assembled with tap water (Kraus and Arduin 1997). The blue aniline dye produces a blue color in callose tissue and Lugol acts on the cell walls, giving a gray and yellowish coloration to lignified areas. The slides containing the histological sections were analyzed and photo documented with an Olympus BX51 light microscope coupled to an Olympus DP175 digital camera (Olympus, Tokyo, Japan) with an ultraviolet filter that emits fluorescence to check for the presence of callose.

Quantitative analyses of anatomical traits (LBT = leaf blade thickness; UET = upper epidermis thickness; LET = lower epidermis thickness; PPT = palisade parenchyma thickness; SPT = spongy parenchyma thickness) were performed based on the measurements of the six leaf histological sections (n = 6), measured five times (6 cuts x 5 measurements) along each photomicrograph using the ImageJ 1.46r program (Rasband 2016).

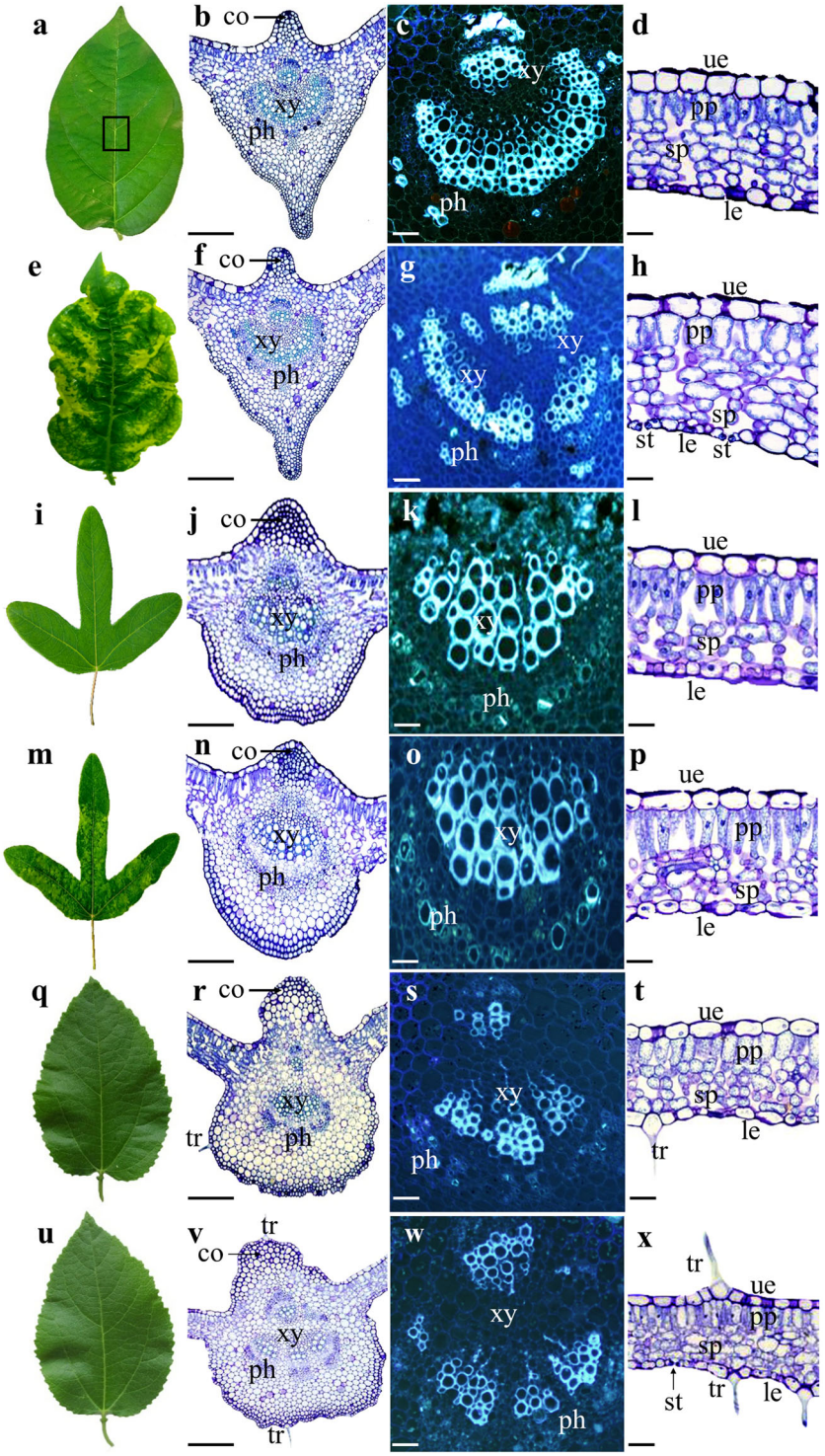

Fig. 2 Light and fluorescence photomicrographs of *Passiflora* leaves. Healthy *P. alata* (**a-d**); *P. alata* infected with CABMV (**e-h**), presenting intense mosaic, blistering and leaf deformation (**e**), with a slight change in the arrangement of the vascular bundles (**f-h**); healthy *P. gibertii* (**i-l**); *P. gibertii* infected with CABMV (**m-p**), presenting light mosaic (**m**) but without alteration in the infected cell structure (**n-p**); healthy *P. malacophylla* (**q-t**); *P. malacophylla* infected with CABMV (**u-x**); symptomies (**u**) and without anatomical modification (**v-x**). co: collenchyma; ue: upper epidermis; le: lower epidermis: pp: palisade parenchyma; sp: spongy parenchyma, tr: trichome, st: stoma. Bar: 500 µm (b, f, j, n, r, v); 200 µm (c, d, g, h, k, l, o, p, s, t, w, x)

Data analysis

The experimental design was completely randomized, distributed in eight treatments (species), with eight replications, in addition to two plants of each species as a control. To determine the disease severity index, control plants of all species and asymptomatic plants of *P. edulis* were not considered in the statistical analyses.

For grouping the species, the DI values (%) were used at 55 DAI according to the Scott-Knott test ($p \leq 0.05$). This grouping was used to categorize the reaction of species in a group based on the DI scale: 0.00 to 10.99% - resistant (R); 11.00 to 25.99% - moderately resistant (MR); 26.00 to 60.99% - susceptible (S); and ≥ 61.00% - highly susceptible (HS). The analysis of the anatomical measurements of *P. edulis* was

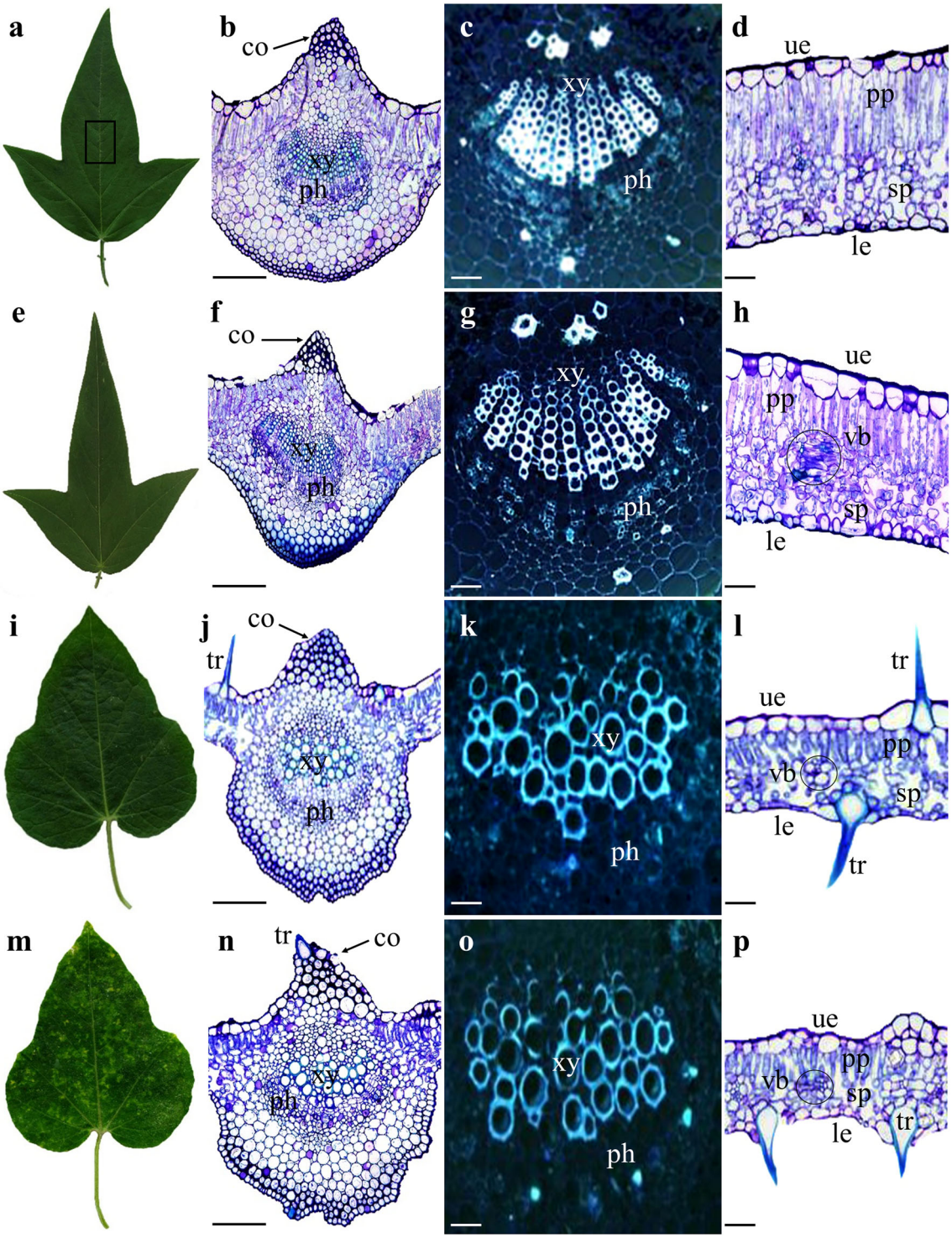

Fig. 3 Light and fluorescence photomicrographs of *Passiflora* leaves. Healthy *P. suberosa* (**a-d**); *P. suberosa* infected with the CABMV (**e-h**) and with normal distribution of infected tissues (**f-h**); healthy *P. foetida* (**i-l**); *P. foetida* infected with CABMV showing symptoms of light mosaic (**m**) and no change in the structures of infected tissues (**n-p**). co: collenchyma; ue: upper epidermis; le: lower epidermis: pp: palisade parenchyma; sp: spongy parenchyma, tr: trichome, st: stoma, vb: vascular bundle. Region of vascular tissue present in the parenchymatic tissue of the leaf (circle). Bar: 500 µm (b, f, j, n); 200 µm (c, d, g, h, k, l, o, p)

enerated according to the different levels of leaf severity (levels 1 to 4, Fig. 1) and box plots were used to visualize the data dispersion. In addition, the control and level 4 (highest level of severity of CABMV) for

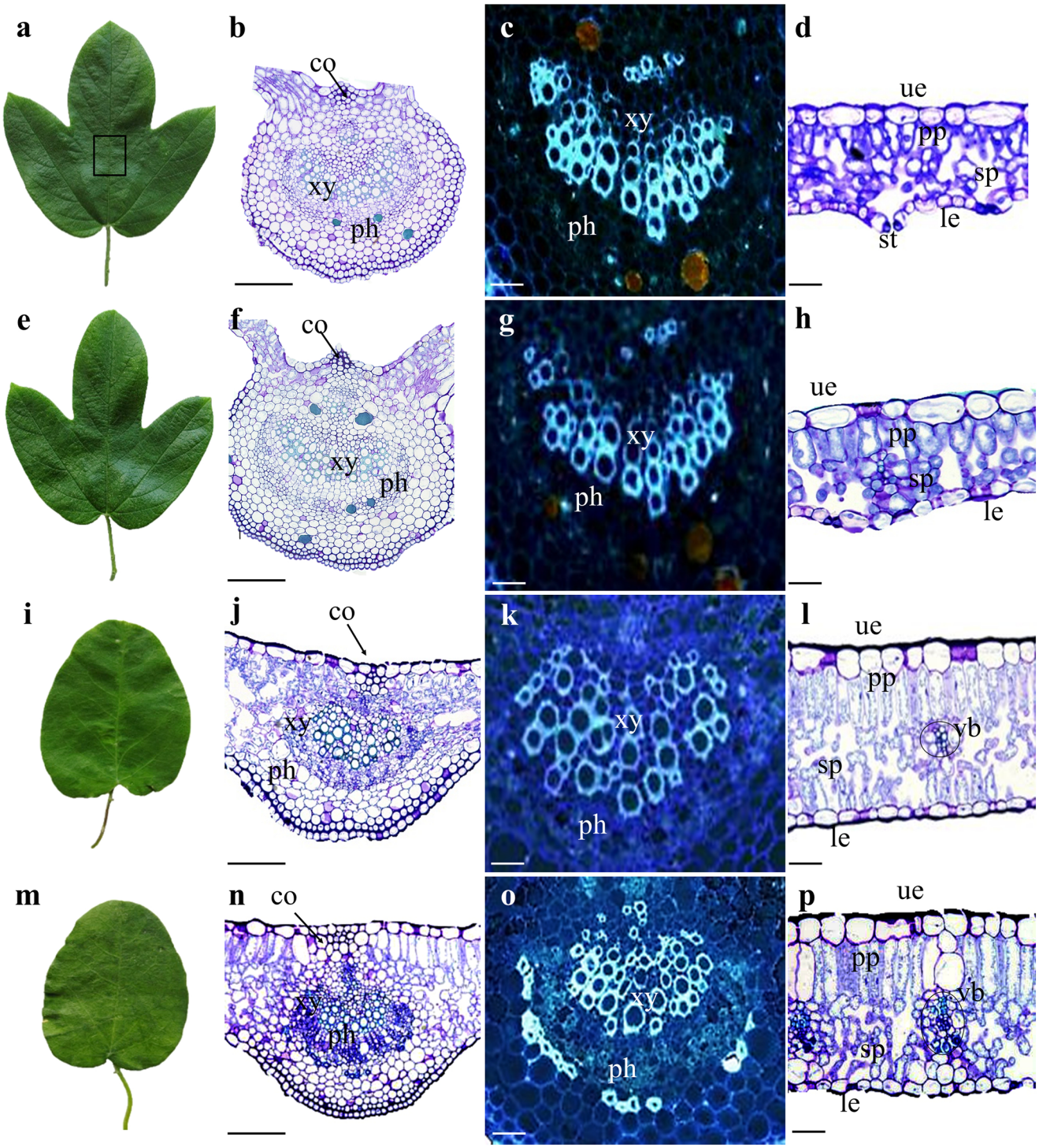

Fig. 4 Light and fluorescence photomicrographs of *Passiflora* leaves. Healthy *P. setacea* (**a-d**); *P. setacea* infected with CABMV (**e-h**) without changes in infected cell tissues (**f-h**); healthy *P. subrotunda* (**i-l**); *P. subrotunda* infected with CABMV (**m-p**), with symptoms of light mosaic (**m**), mild cell disorganization and prominent palisade parenchyma in the leaf mesophyll region (**n-p**). co: collenchyma, ph: phloem, xy: xylem, ue: upper epidermis, le: lower epidermis, pp: palisade parenchyma, sp: spongy parenchyma, tr: trichome, vb: vascular bundle, st: stoma. Bar: 500 µm (**b, f, j, n**), 200 µm (**c, d, g, h, k, l, o, p**)

this species were analyzed as positive controls. The anatomical trait data of the other *Passiflora* species were subjected to analysis of variance and compared by the F-test ($p \leq 0.05$). All statistical analyses were performed using the 'agricolae' package in the R program (R Development Core Team 2020).

Results

Severity classification of passion fruit species to CABMV

The transmission electron microscopy (TEM) analysis performed on the parenchyma of the apical leaves of the *P. edulis* plants without infection, as expected, did not show viral structures in the transmission electron photomicrographs (Supplementary Fig. 1a). Plants with typical symptoms of CABMV (Supplementary Fig. 1b), used for mechanical inoculation of species (Table 1), showed the presence of cylindrical inclusions typical of viruses of the genus *Potyvirus* (Supplementary Fig. 1b).

The CABMV severity in the species evaluated ranged from 0.0–58.2%, according to the disease index (DI) at 55 DAI. Among the species evaluated, *P. suberosa* (BGP014), *P. setacea* (BGP238), *P. malacophylla* (BGP170) and *P. gibertii* (BGP414) were classified as resistant, with DI ranging from 0.0–2.4%. In contrast, the species *P. alata* (BGP393) and *P. edulis* (BRS Gigante Amarelo), were classified as susceptible, with DI values of 58.2% and 51.9%, respectively (Table 1).

Anatomical alterations of passion fruit species infected with CABMV

In the controls, normal tissue distribution was observed in the eight species of *Passiflora*. Four species infected with CABMV (*P. foetida*, *P. subrotunda*, *P. alata* and *P. edulis*) presented different variations of leaf symptoms (from light mosaic to leaf deformations) and changes in the distribution of the internal leaf tissues *P. gibertii*, had mild symptoms of CABMV and did not present any alteration in cell structures.

Table 1 Incidence, minimum, maximum and average value of severity and classification of passion fruit species artificially infected with *cowpea aphid-borne mosaic virus* (CABMV)

Species	Code	Inc. (%)	Min.	Max.	DI (%)[1]	Class [2]
P. edulis	BRS-GA*	100	3.8	59.9	51.9 a	S
P. alata	BGP393	100	20.9	61.8	58.2 a	S
P. subrotunda	BGP394	62	0.0	33.3	18.8 b	MR
P. foetida	BGP395	85	9.0	33.3	20.0 b	MR
P. gibertii	BGP414	14	0.0	8.5	2.4 c	R
P. malacophylla	BGP170	0.0	0.0	0.0	0.0 c	R
P. setacea	BGP238	0.0	0.0	0.0	0.0 c	R
P. suberosa	BGP014	0.0	0.0	0.0	0.0 c	R

* BRS-GA = BRS Gigante Amarelo

[1] DI = Disease index at 55 DAI

[2] R = Resistant; MR = moderately resistant; S = susceptible

Similarly, infected *P. malacophylla, P. setacea* and *P. suberosa* also showed no changes in cell structures, without symptoms of the disease (Figs. 1, 2, 3 and 4).

The anatomical analyses in *P. edulis* (Fig. 1a-t) allowed the identification of major anatomical changes in this species as the symptoms of passion fruit woodiness disease progressed, including reduction of parenchymal tissues and alteration in the distribution of vascular bundles in the central vein of the leaves. The control plants did not have morphological (Fig. 1a) or anatomical (Fig. 1b-d) alterations. Greater thickness of the collenchyma in the central vein (Fig. 1f) was observed in *P. edulis* plants without (level 1) infection severity (Fig. 1e-h). Similar behavior was also observed at the other levels of disease severity (Fig. 1j, n, r).

Changes in the arrangement of the vascular bundles were observed only after level 3 (Fig. 1n-o). The xylem and phloem vessels were disassociated from their natural conformation forming three vascular bundles (Fig. 1n), more visibly with fluorescence microscopy (Fig. 1o). This observation was more evident in the greatest degree of severity (level 4), in which the leaves had intense mosaic formation, blistering and deformation. In addition, the presence of four vascular bundles was observed at this severity level, in addition to reduction in the diameter of the xylem vessels (Fig. 1r, s).

Palisade and spongy parenchyma tissues of *P. edulis* were also reduced when infected with CABMV. This also occurred in the leaves that did not show visual symptoms of the disease (Fig. 1h). Additionally, the cells of the spongy parenchyma showed deformations and hypertrophy in the shape of the cells, hypertrophy and depressions in certain regions of the leaf blade with the progression of the symptoms of the disease (Fig. 1p, t) compared to the control (Fig. 1d).

In the control plants of *P. alata*, as well as all six wild *Passiflora* species evaluated, the presence of leaf mosaic was not observed (Figs. 2a, i and q, 3a and i and 4a and i). Plants infected with CABMV, on the other hand, showed some degree of viral infection (Fig. 2e, m, 3m, 4m) except for *P. malacophylla* (Fig. 2u), *P. suberosa* (Fig. 3e) and *P. setacea* (Fig. 4e), which did not show symptoms of CABMV.

In *P. alata*, no significant anatomical changes were seen after inoculation, instead only the start of dissociation in the arrangement of the vascular bundles (Fig. 2f-g) when compared to the control treatment (Fig. 2b-c). The palisade parenchyma was not altered due to the manifestation of symptoms, whereas the spongy parenchyma showed slight hypertrophy when infected (Fig. 2h).

In *P. gibertii*, anatomical changes in the distribution of vascular bundles were not seen. On the other hand, the xylem vessels had altered disposition, mainly when analyzed by fluorescence microscopy (Fig. 2). Similarly, in *P. malacophylla* there was also a slight change in the arrangement of the vascular bundle of the central vein observed both by light and

fluorescence microscopy (Fig. 2v, x). Despite the leaf anatomical changes observed in this species, no visual symptoms were observed in the leaves, so they were classified as resistant to the virus.

In relation the anatomical analyses in *P. suberosa*, there were no changes in the central vein and leaf mesophyll between the infected and control plants (Fig. 3b, f). This species presented the largest palisade and spongy parenchyma, which may be associated with resistance to passion fruit woodiness disease (Fig. 3d, h). *P. foetida* also showed no anatomical changes in plants infected with CABMV (Fig. 3m-p), although mild symptoms of the disease were observed in this species, classified as moderately resistant (Table 1). In addition, the presence of trichomes in the abaxial and adaxial surfaces was observed in the leaves of the control and infected plants (Fig. 3l, p).

In *P. setacea* (classified as resistant, DI = 0.0%), no anatomical changes associated with the virus were identified, with the presence of phenolic compounds in the region of the central vein of the control and infected leaves (Fig. 4a-h). The species *P. subrotunda*, classified as moderately resistant, (DI = 18.8%), showed similarity between the control and infected treatments in the distribution of the tissues of the central vein (Fig. 4j, n), but a reduction in the spongy parenchyma of the infected plants was observed with greater agglutination of cells in this region in relation to the control plants, in which the cells were well spaced, facilitating gas exchange (Fig. 4l, p).

Considering the morphoanatomical analyses of *P. edulis* in relation to viral infection, significant hypertrophy ($p \leq 0.05$) was observed in the leaf blade of plants infected with and without CABMV symptoms in relation to the control treatment (Fig. 5a).

The upper epidermis thickness was not affected by the severity of passion fruit woodiness disease (Fig. 5b). The dispersion of the morphoanatomical data indicates that leaves without (level 1) and with lower severity level (level 2) showed greater amplitude in the distribution of data in relation to the control plants (Fig. 5).

Based on the morphoanatomical analyses of *P. edulis* control plants and the highest severity of CABMV (level = 4), significant reductions ($p \leq 0.05$) were observed in the leaf blade thickness (Fig. 6a), lower epidermis (Fig. 6c) palisade parenchyma (Fig. 6d) and spongy (Fig. 6e), with reductions of 24.5%, 13.9%, 18.6% and 34.8% compared to the control treatments, respectively. The upper epidermis thickness of *P. edulis* remained unchanged (Fig. 6b).

In *P. alata*, significant anatomical changes were observed due to inoculation with CABMV ($p \leq 0.05$) for all the traits except LET and PPT. This species, together with *P. edulis*, had the highest incidence and severity of CABMV according to the disease index (Table 1). The leaf blade thickness (Fig. 6f), upper epidermis (Fig. 6g) and spongy parenchyma (Fig. 6j) of *P. alata* plants subjected to infection with CABMV was significantly reduced by 23.3%, 24.7% and 34.7%, compared to the control treatment, respectively.

In *P. foetida*, only the spongy parenchyma thickness ($p \leq 0.05$) changed after infection with the virus, with an increase of 11.9% compared to the control treatment (Fig. 6). The morphological and anatomical evaluation of *P. gibertii* showed the opposite behavior to *P. alata* and *P. edulis*, with hyperplasia of the leaf blade (Fig. 6p), palisade parenchyma (Fig. 6s) and spongy parenchyma (Fig. 6t), in thickness increases of 16.6%, 13.2% and 21.9% in the infected plants compared to the controls, respectively. A change in the lower epidermis thickness was also observed, with a significant reduction ($p \leq 0.05$) of 13.7% in the infected plants (Fig. 6r).

In *P. malacophylla*, there was morphometric alteration of the anatomical traits LBT (Fig. 6u) and PPT (Fig. 6x) when the plants were infected with CABMV, with increases of 16.6% and 22.1%, in relation to their respective controls. In relation to *P. setacea*, plants infected by the virus showed a significant increase ($p \leq 0.01$) of 16% in LET compared to the control plants (Fig. 6ab). For the other morphometric traits evaluated, there were no differences ($p > 0.05$) between the infected and non-infected plants of *P. setacea* (Fig. 6z, aa, ac, ad).

The leaves of *P. suberosa* did not show CABMV symptoms, but a significant reduction ($p \leq 0.01$) of PPT was observed in the presence of the virus, with 20.9% less than the control plants (Fig. 6ah). There was no change for the other traits between infected and non-infected plants of *P. suberosa* (Fig. 6ae, af, ag, ai). The leaves of *P. subrotunda* showed hypertrophy in the spongy parenchyma ($p \leq 0.05$), 16.5% lower in the infected plants compared to the controls (Fig. 6an). The other traits did not differ significantly ($p \geq 0.05$) (Fig. 6aj, ak, al, am). The presence of light mosaic on the leaves of *P. subrotunda* was not enough to significantly alter the anatomical structures of the infected plants in relation to the controls.

Discussion

The wild species of passion fruit that showed complete resistance (ID = 0.0%) to CABMV in our study are natural sources of resistance and/or tolerance genes, both to biotic (Gonçalves et al. 2018) and abiotic factors (Souza et al. 2018; Lima et al. 2020). Studies carried out by several authors have also reported that the wild species *P. setacea, P. suberosa* and *P. malacophylla* (Oliveira et al. 2013; Freitas et al. 2015, 2016; Santos et al. 2015a; Gonçalves et al. 2018; Sacoman et al. 2018) present complete resistance to CABMV, so they can be used in interspecific hybridizations to obtain new resistant cultivars. Santos et al. (2015a) demonstrated success in obtaining 156 interspecific hybrids from the cross between *P. edulis* x *P. setacea*, of which 25 were considered resistant

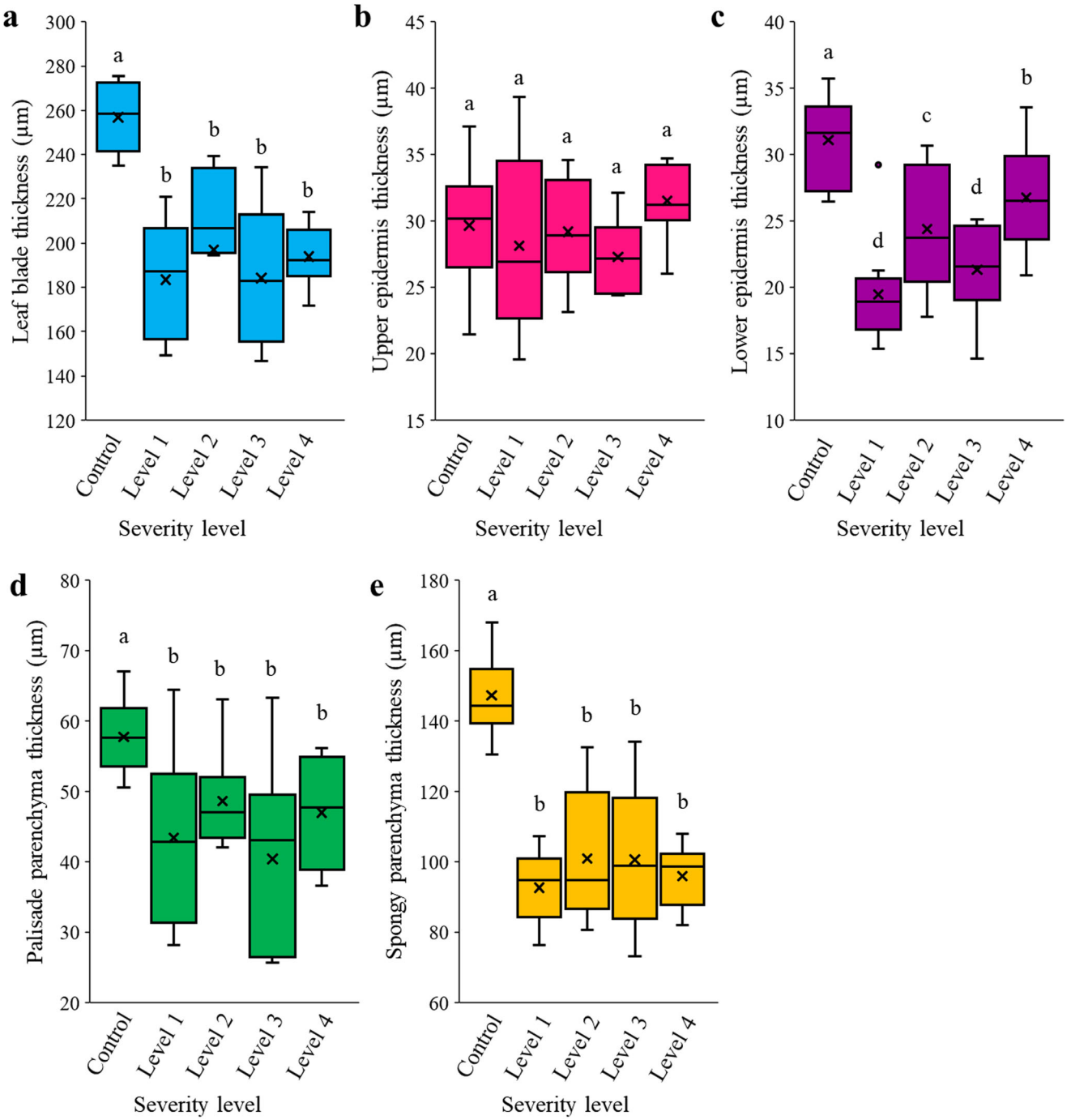

Fig. 5 Box plots of the anatomical traits of *Passiflora edulis* plants infected with CABMV. The line shown in the box is the median value and the x indicates the average of the data. Different letters on the top whiskers indicate statistically different means (Scott-Knott test, $p \leq 0.05$)

to CABMV in field conditions. Other authors have also reported resistance of *P. setacea* to CABMV (Oliveira et al. 2013; Gonçalves et al. 2018).

Despite the immunity observed in *P. suberosa* to CABMV, this species belongs to the subgenus Decaloba (2n = 24; 36) (Melo et al. 2016), while *P. edulis* belongs to the subgenus *Passiflora* (2n = 18) (Melo et al. 2016; Pamponét et al. 2019). The lack of chromosomal homology between these two subgenera makes it difficult to obtain interspecific hybrids resistant to CABMV under natural conditions. Although, studies demonstrate success in obtaining interspecific hybrids of *Passiflora* even in the absence of chromosomal homology (Soares et al. 2015; Soares et al. 2018). This probably occurred because interspecific barriers of incompatibility in *Passiflora* are relatively fragile (Meletti et al. 2005).

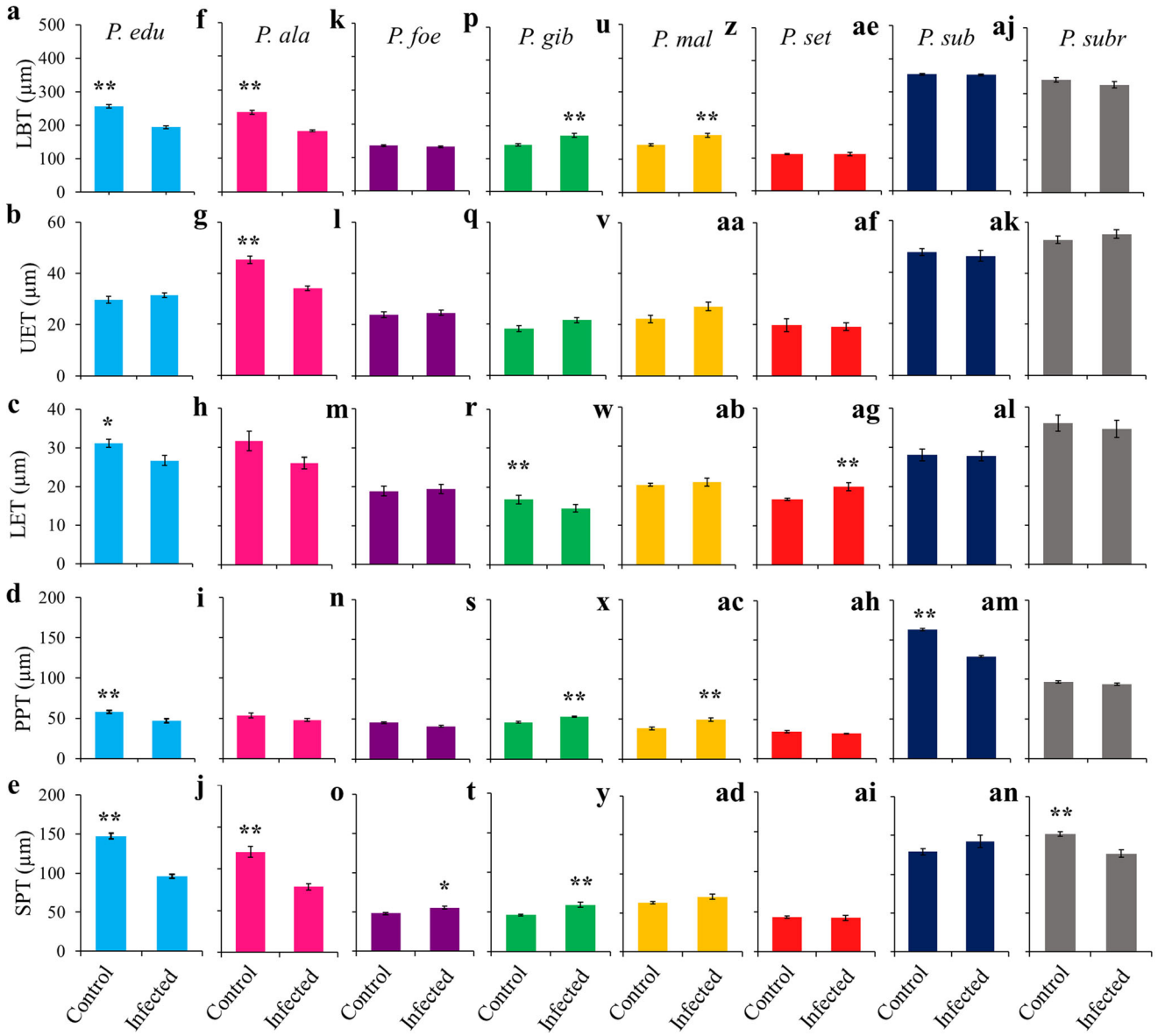

Fig. 6 Quantitative anatomical traits of *Passiflora* species with the passion fruit woodiness disease: *P. edu: P. edulis*, *P. ala*: *P. alata*, *P. foe*: *P. foetida*, *P. gib: P. gibertii*, *P. mal: P. malacophylla*, *P. set: P. setacea*, *P. sub: P. suberosa* and *P. subr*: *P. subrotunda*. (**), (*) The top of the error bars indicates statistically different means according to the F-test at 1 and 5% probability. LBT: leaf blade thickness; UET: upper epidermis thickness; LET: lower epidermis thickness; PPT: palisade parenchyma thickness; SPT: spongy parenchyma thickness

It is interesting to note that the species *P. malacophylla* considered resistant to CABMV can be used in hybridization programs to transfer resistance alleles to commercial species (*P. edulis*), since both have the same number of chromosomes (2n = 18) (Souza et al. 2003; Pamponét et al. 2019), increasing the chances of obtaining commercial hybrids tolerant to CABMV.

Several authors have reported anatomical changes in different species of plants infected by viruses (Takimoto et al. 2009; Gomes et al. 2010), including *Passiflora* species (Gonçalves et al. 2018). Viral infection is a controlled and multifaceted process, in which the virus appropriates the host's cell functions to replicate itself (Netherton and Wileman 2011; Niehl and Heinlein 2011). We found that *P. edulis* showed the greatest morphological and anatomical changes in the leaves, with a potential impact on plant metabolism by reducing leaf expansion and production of photoassimilates (Bolton 2009; Fernández-Calvino et al. 2014; Murray et al. 2016). As symptoms progressed, changes in cell conformation and vascular bundles became more pronounced in symptomatic plants of *P. edulis* (Figs. 1 and 5).

Morphoanatomical measurements were also affected by CABMV in asymptomatic plants (Fig. 5), indicating that the virus promotes changes in the anatomical structure of the leaves even in the absence of visible symptoms. Although there was no mosaic or deformation, there was apparent

chlorosis in asymptomatic plants (Fig. 1e), indicating some physiological disorder caused by the presence of the virus. In this respect, *Vitis vinifera* L. plants infected with tomato ringspot virus (ToRSV) showed chlorotic leaves, without leaf deformation, but with changes in the cytoplasm, chloroplasts, nucleus, cell wall, xylem and phloem. ToRSV mainly affected chloroplasts, with deformation in thylakoids, accumulation of starch granules and vacuolar deformation (El-Banna et al. 2014). Further studies are essential to associate these anatomical changes (Fig. 5) with molecular and or enzymatic aspects of *Passiflora edulis*.

The fluorescence microscope technique to identify callose compounds from the plant-virus interaction was not effective, since there was no difference between the control and the infected plants. Callose is deposited on the plasma membrane and cell wall after mechanical, chemical, physiological or biotic damage (Chen and Kim 2009). In addition, no induction of defense associated with the formation of calcium oxalate crystals, tylosis and high deposition of callose in the xylem and phloem vessels was observed, which would prevent the virus from colonizing vascular tissue. It is important to mention that this response induction is more common in plant-fungus interactions (Ellinger and Voigt 2014; Lima et al. 2019).

Anatomical changes directly interfere with the cell wall structure and/or the conformation and distribution of organelles, thereby altering the biochemical processes of signaling and synthesis and impacting productivity (Grove and Marsh 2011; El-Banna et al. 2014; Xiao et al. 2016).

In this study, viral infection caused greater anatomical change at the level of the spongy parenchyma, reducing the intercellular spaces in *P. edulis*, *P. alata* (classified as susceptible) and in *P. subrotunda* (classified as moderately resistant). This region of the mesophyll is fundamental for physiological functioning, because it is where the gas exchange takes place between the stomatal chamber and the external environment (Xiao et al. 2016). The probable consequence is reduction in the photosynthetic rate of the plant (Su et al. 2018).

The anatomical changes observed in our study were directly associated with CABMV severity, considering that greater changes in tissue conformation and dimensions were observed in *P. edulis* and *P. alata*, while the other species, such as *P. suberosa*, *P. gibertii* and *P. malacophylla*, showed only slight changes in the dimensions of the infected tissues, confirming the results obtained by Gonçalves et al. (2018). Virus resistance involves a series of physiological, biochemical, anatomical, molecular and genetic processes (Alexander and Cilia 2016). Therefore, knowing the mechanisms associated with viral infection is essential to better understand the plant-pathogen interaction. Furthermore, it is important to understand the molecular processes that affect resistance to CABMV in *Passiflora* spp. through further investigation of *Passiflora* x CABMV interaction.

Based on the severity of the disease, it was possible to identify resistance to CABMV in the wild species *P. malacophylla*, *P. setacea* and *P. suberosa*. These species did not show leaf symptoms and changes in the arrangement of cell structures when infected by CABMV, showing potential for use in interspecific hybridizations with susceptible commercial species (*P. edulis* and *P. alata*) or use of other unconventional breeding strategies. The species *P. subrotunda* and *P. foetida* were classified as moderately resistant to CABMV, with slight anatomical disorganization. Viral infection directly affected the distribution and organization of vascular bundles and spongy parenchyma hypertrophy in *P. edulis* and *P. alata*. Considering the different levels (1 to 4) of severity of CABMV in *P. edulis*, viral infection promoted changes in leaf anatomy even in asymptomatic plants (level 1) and major anatomical changes occurred as the symptoms of disease progressed, including parenchyma tissue reduction (level 2) and complete change in the arrangement of vascular bundles (phloem and xylem) in the central leaf vein (levels 3 and 4).

Supplementary Information The online version contains supplementary material available at https://doi.org/10.1007/s13313-020-00763-z.

Acknowledgements The Coordenação de Aperfeiçoamento de Pessoal de Nível Superior (CAPES) provided a doctoral research grant to the first author (Z.S.G) and postdoctoral research grants to the third author (T.L.S – PNPD/UEFS 15950830814) and fourth author (E.H.S – PNPD 88882.315208/2019-01). The Conselho Nacional de Desenvolvimento Científico e Tecnológico (CNPq) provided a postdoctoral scholarship to the second author (L.K.S.L – PDJ 152109/2019-6), financial support (Process 421033/2018-5) and a research productivity fellowship to the fifth author (O.N.J. – PQ312774/2018-4). The Embrapa Mandioca e Fruticultura research unit provided the plant material along with experimental, technical and financial support (Process 22.16.04.007.00.00). Professor Elliot Watanabe Kitajima and the Nucleus for Electronic Microscopy of the Universidade de São Paulo (Esalq-USP) supported the processing of samples for transmission electron microscopy.

Compliance with ethical standards

Conflict of interest The authors declare no conflict of interest.

References

Alexander MM, Cilia M (2016) A molecular tug-of-war: global plant proteome changes during viral infection. Curr Plant Biol 5:13–24. https://doi.org/10.1016/j.cpb.2015.10.003

Andersen EJ, Ali S, Byamukama E, Yen Y, Nepal MP (2018) Disease resistance mechanisms in plants. Genes 9:1–30. https://doi.org/10.3390/genes9070339

Bolton MD (2009) Primary metabolism and plant defense: fuel for the fire. Mol Plant Microbe Interact 22:487–449. https://doi.org/10.1094/MPMI-22-5-0487

Boutrot F, Zipfel C (2017) Function, discovery, and exploitation of plant pattern recognition receptors for broad-spectrum disease resistance.

Annu Rev Phytopathol 55:257–286. https://doi.org/10.1146/annurev-phyto-080614-120106

Cai Y, Cai X, Wang Q, Wang P, Zhang Y, Cai C, Geng S (2020) Genome sequencing of the australian wild diploid species *Gossypium australe* highlights disease resistance and delayed gland morphogenesis. Plant Biotechnol J 18:814–828. https://doi.org/10.1111/pbi.13249

Carvalho BM, Viana AP, Santos PHD, Generoso AL, Corrêa CCG, Silveira V, Santos EA (2019) Proteome of resistant and susceptible *Passiflora* species in the interaction with *Cowpea aphid-borne mosaic virus* reveals distinct responses to pathogenesis. Euphytica 215: 1–17. https://doi.org/10.1007/s10681-019-2491-5

Chen XY, Kim JY (2009) Callose synthesis in higher plants. Plant Signal Behav 4:489–492. https://doi.org/10.4161/psb.4.6.8359

El-Banna OHM, Awad MA, Abbas MS, Waziri HM, Darwish HS (2014) Anatomical and ultrastructural changes in tomato and grapevine leaf tissues infected with tomato ringspot virus. Egyptian J Virol 11: 102–111

Ellinger D, Voigt CA (2014) The use of nanoscale fluorescence microscopic to decipher cell wall modifications during fungal penetration. Front Plant Sci 5:1–6. https://doi.org/10.3389/fpls.2014.00270

Fernández-Calvino L, Osorio S, Hernández ML, Hamada IB, Del Toro FJ, Donaire L, Yu A, Bustos R, Fernie AR, Martínez-Rivas JM, Llave C (2014) Virus-induced alterations in primary metabolism modulate susceptibility to *Tobacco rattle virus* in Arabidopsis. Plant Physiol 166:1821–1838. https://doi.org/10.1104/pp.114.250340

Freitas JCO, Viana AP, Santos EA, Silva FH, Paiva CL, Rodrigues R, Souza MM, Eiras M (2015) Genetic basis of the resistance of a passion fruit segregant population to *Cowpea aphid borne mosaic virus* (CABMV). Trop Plant Pathol 40:291–297. https://doi.org/10.1007/s40858-015-0048-2

Freitas JCO, Viana AP, Santos EA, Paiva CL, Silva FHL, Souza MM (2016) Sour passion fruit breeding: Strategy applied to individual selection in segregating population of *Passiflora* resistant to *Cowpea aphid-born mosaic virus* (CABMV). Sci Hortic 211:241–247. https://doi.org/10.1016/j.scienta.2016.09.002

Garcêz RM, Chaves ALR, Eiras M, Meletti LMM, Azevedo Filho JA, Silva LA, Colariccio A (2015) Survey of aphid population in a yellow passion fruit crop and its relationship on the spread *Cowpea aphid borne mosaic virus* in a subtropical region of Brazil. Springerplus 4:1–12. https://doi.org/10.1186/s40064-015-1263-5

Gomes RT, Kitajima EW, Tanaka FAO, Marques JPR, Appezzato-Glória B (2010) Anatomia de lesões foliares causadas pelo vírus da Mancha Clorótica do Clerodendrum, transmitido pelo ácaro *Brevipalpus phoenicis* em diferentes espécies. Summa Phytopathol 36:291–297. https://doi.org/10.1590/S0100-54052010000400003

Gonçalves ZS, Lima LKS, Soares TL, Abreu EFM, Barbosa CJ, Cerqueira-Silva CBM, Jesus ON, Oliveira EJ (2018) Identification of *Passiflora* spp. genotypes resistant to *Cowpea aphid-borne mosaic virus* and leaf anatomical response under controlled conditions. Sci Hortic 231:166–178. https://doi.org/10.1016/j.scienta.2017.12.008

Gouveia BC, Calil IP, Machado JPB, Santos AA, Fontes EP (2017) Immune receptors and co-receptors in antiviral innate immunity in plants. Front Microbiol 7:1–14. https://doi.org/10.3389/fmicb.2016.02139

Grove J, Marsh M (2011) The cell biology of receptor-mediated virus entry. J Cell Biol 195:1071–1082. https://doi.org/10.1083/jcb.201108131

Hinch JM, Clarke AE (1982) Callose formation in *Zea mays* as a response to infection with *Phytophthora cinnamomi*. Physiol Plant Pathol 21: 113–124. https://doi.org/10.1016/0048-4059(82)90014-5

IBGE - Instituto Brasileiro de Geografia e Estatística (2020) Survey of national passion fruit production in the year 2018. https://sidra.ibge.gov.br/tabela/5457/. Accessed 18 Mar 2020

Jesus ON, Soares TL, Oliveira EJ, Santos TCP, Farias DH, Bruckner CH, Novaes QS (2016) Dissimilarity based on morphological characterization and evaluation of pollen viability and in vitro germination in *Passiflora* hybrids and backcrosses. Acta Hortic 29:401–408. https://doi.org/10.17660/ActaHortic.2016.1127.62

KitajimA EW, Alcantara BK, Madureira PM, Alfenas-Zerbini P, Rezende JAM, Zerbini FM (2008) A mosaic of beach bean (*Canavalia rosea*) caused by an isolate of *Cowpea aphid-borne mosaic virus* (CABMV) in Brazil. Arch Virol 153:743–747. https://doi.org/10.1007/s00705-008-0052-7

Kraus JR, Arduin M (1997) Basic manual of methods in plant morphology. Eduar, Rio de Janeiro

Lima LKS, Jesus ON, Soares TL, Oliveira SAS, Haddad F, Girardi EA (2019) Water deficit increases the susceptibility of yellow passion fruit seedlings to Fusarium wilt in controlled conditions. Sci Hortic 243:609–621. https://doi.org/10.1016/j.scienta.2018.09.017

Lima LKS, Jesus ON, Soares TL, Santos IS, Oliveira EJ, Coelho Filho MA (2020) Growth, physiological, anatomical and nutritional responses of two phenotypically distinct passion fruit species (*Passiflora* L.) and their hybrid under saline conditions. Sci Hortic 263:2–15. https://doi.org/10.1016/j.scienta.2019.109037

Mckinney HH (1923) Influence of soil temperature and moisture on infection of wheat seedlings by *Helminthosporium sativum*. J Agric Res 26:195–218

Meletti LMM, Soares-Scott MD, Bernacci LC, Passos IRS (2005) Melhoramento genético do maracujá: passado e futuro. In: Faleiro FG, Junqueira NTV, Braga MF (eds) Maracujá: germoplasma e melhoramento genético. Embrapa Cerrados, Planaltina, pp 55–78

Melo CAF, Souza MM, Viana AP, Santos EA, Oliveira Souza V, Corrêa RX (2016) Morphological characterization and genetic parameter estimation in backcrossed progenies of *Passiflora* L. for ornamental use. Sci Hortic 212:91–103. https://doi.org/10.1016/j.scienta.2016.08.013

Murray RR, Emblow MS, Hetherington AM, Foster GD (2016) Plant virus infections control stomatal development. Sci Rep 6:1–7. https://doi.org/10.1038/srep34507

Netherton CL, Wileman T (2011) Virus factories, double membrane vesicles and viroplasm generated in animal cells. Curr Opin Virol 1: 381–387. https://doi.org/10.1016/j.coviro.2011.09.008

Niehl A, Heinlein M (2011) Cellular pathways for viral transport through plasmodesmata. Protoplasma 248:75–99. https://doi.org/10.1007/s00709-010-0246-1

Novaes QS, Rezende JAM (2003) Selected mild strains of *Passion fruit woodiness virus* (PWV) fail to protect preimmunized vines in Brazil. Sci Agric 60:699–708. https://doi.org/10.1590/S0103-90162003000400014

Oliveira EJ, Soares TL, Barbosa CDJ, Santos-Filho HP, Jesus ON (2013) Disease severity from passion fruit to identify sources of resistance in field conditions. Rev Bras Frut 35:485–492. https://doi.org/10.1590/S0100-29452013000200018

Palomares-Rius JE, Escobar C, Cabrera J, Vovlas A, Castilla P (2017) Anatomical alterations in plant tissues induced by plant-parasitic Nematodes. Front Plant Sci 8:1–16. https://doi.org/10.3389/fpls.2017.01987

Pamponét VCC, Souza MM, Silva GS, Micheli F, Melo CAF, Oliveira SG, Corrêa RX (2019) Low coverage sequencing for repetitive DNA analysis in *Passiflora edulis* Sims: citogenomic characterization of transposable elements and satellite DNA. BMC Genomics 262:1–17. https://doi.org/10.1186/s12864-019-5576-6

Preisigke SDC, Viana AP, Santos EA, Santos PRD, Santos VOD, Ambrósio M, Walter FHDB (2020) Selection strategies in a segregating passion fruit population aided by classic and molecular

techniques. Bragantia 79:1–15. https://doi.org/10.1590/1678-4499.20190291

R Core Team (2020) R: A language and environment for statistical computing. R Foundation for Statistical Computing, Vienna

Rai AK, Basavaraj YB, Sadashiva AT, Krishna M, Reddy M, Ravishankar KV, Hussain Z, Venugopalan R, Reddy MK (2020) Evaluation of tomato genotypes for resistance to bud necrosis disease caused by groundnut bud necrosis virus (GBNV). Crop Prot 131:1–8. https://doi.org/10.1016/j.cropro.2019.105074

Rasband WS (2016) ImageJ. U S National Institutes of Health, Bethesda

Sacoman NN, Viana AP, Carvalho VS, Santos EA, Rodrigues R (2018) Resistance to *Cowpea aphid-borne mosaic virus* in *in vitro* germinated genotypes of *Passiflora setacea*. Rev Bras Frut 40:1–10. https://doi.org/10.1590/0100-29452017607

Sade D, Sade N, Brotman Y, Czosnek H (2020) Tomato yellow leaf curl virus (TYLCV)-resistant tomatoes share molecular mechanisms sustaining resistance with their wild progenitor *Solanum habrochaites* but not with TYLCV-susceptible tomatões. Plant Sci 110439:1–6. https://doi.org/10.1016/j.plantsci.2020.110439

Santos EA, Viana AP, Freitas JCO, Rodrigues DL, Ferreira RT, Paiva CL, Souza MM (2015b) Genotype selection by REML/BLUP methodology in a segregating population from an interspecific *Passiflora* spp. crossing. Euphytica 204:1–11. https://doi.org/10.1007/s10681-015-1367-6

Santos EA, Viana AP, Oliveira FJC, Lima FH, Rodrigues RAND, Eiras M (2015a) Resistance to *Cowpea aphid borne mosaic virus* in species and hybrids of *Passiflora*: advances for the control of the passion fruit woodiness disease in Brazil. Eur J Plant Pathol 143:85–98. https://doi.org/10.1007/s10658-015-0667-y

Santos VOD, Viana AP, Preisigke SDC, Santos EA (2019) Characterization of a segregating population of passion fruit with resistance to *Cowpea aphid borne mosaic virus* through morpho-agronomic descriptors. Gen Mol Res 18:1–13. https://doi.org/10.4238/gmr18255

Soares TL, Jesus ON, Souza EHAND, Oliveira EJ (2015) Reproductive biology and pollen–pistil interactions in *Passiflora* species with ornamental potential. Sci Hortic 197:339–349. https://doi.org/10.1016/j.scienta.2015.09.045

Soares TL, Jesus ON, Souza EH, Oliveira EJ (2018) Floral development stage and its implications for the reproductive success of *Passiflora* L. Sci Hortic 238:333–342. https://doi.org/10.1016/j.scienta.2018.04.034

Souza MM, Pereira TNS, Silva LC, Reis DSS, Sudré CP (2003) Karyotype of six *Passiflora* species collected in the state of Rio de Janeiro. Cytologia 68:165–171. https://doi.org/10.1508/cytologia.68.165

Souza PU, Lima LKS, Soares TL, Jesus ON, Coelho Filho MA, Girardi EA (2018) Biometric, physiological and anatomical responses of *Passiflora* spp. to controlled water deficit. Sci Hortic 229:77–90. https://doi.org/10.1016/j.scienta.2017.10.019

Spadotti DMDA, Favara GM, Novaes QS, Mello APOA, Freitas DMS, Edwards Molina JPAND, Rezende JAM (2019) Long lasting systematic roguing for effective management of CABMV in passion flower orchards through maintenance of separated plants. Plant Pathol 68:1259–1267. https://doi.org/10.1111/ppa.13054

Su J, Yang L, Zhu Q, Wu H, He Y, Liu Y, Zhang S (2018) Active photosynthetic inhibition mediated by MPK3/MPK6 is critical to effector-triggered immunity. PLoS Biol 16:1–29. https://doi.org/10.1371/journal.pbio.2004122

Takimoto JK, Queiroz-Voltan RB, Souza-Dias JACD, Cia E (2009) Alterações anatômicas em algodoeiro infectado pelo vírus da doença azul. Bragantia 68:109–116. https://doi.org/10.1590/S0006-87052009000100012

Xiao Y, Tholen D, Zhu XG (2016) The influence of leaf anatomy on the internal light environment and photosynthetic electron transport rate: exploration with a new leaf ray tracing model. J Exp Bot 67:6021–6035. https://doi.org/10.1093/jxb/erw359

Xiao D, Duan X, Zhang M, Sun T, Sun X, Li F, Wang D (2018) Changes in nitric oxide levels and their relationship with callose deposition during the interaction between soybean and soybean mosaic virus. Plant Biol 20:318–326. https://doi.org/10.1111/plb.12663